

# Progress in measuring GMR in unstable nuclei: Decay detector calibration and inverse reaction experiment

J. Button, Y.-W. Lui, and D.H. Youngblood

## I. Introduction

The Giant Monopole Resonance (GMR) is interesting because its excitation energy is directly related to the incompressibility of the nucleus  $K_A$ .  $K_A$  can be used to derive the incompressibility of nuclear matter  $K_{NM}$ , but this extrapolation from the data for real nuclei is not straightforward due to contributions from surface, Coulomb and asymmetry effects. Thus, improvements to the extrapolated  $K_{NM}$  can be made by measuring the GMR for increasing asymmetry  $(N-Z)/A$ . The incompressibility of nuclear matter is of importance in the nuclear equation of state (EOS) which describes a number of phenomena: collective excitations of nuclei, supernova explosions and radii of neutron stars [1]. The GMR and nuclear incompressibility provide important tests for nuclear effective forces. Additionally, measurement of the ISGMR along isotopic chains with changing nuclear pairing effects may be a useful tool for demonstrating whether or not superfluidity has an effect on nuclear incompressibility [2].

The measurement of the GMR in unstable nuclei was done using inverse kinematics, with a 40 MeV per nucleon beam of the unstable nucleus incident on a  ${}^6\text{Li}$  target. X. Chen *et al.* studied the viability of this approach, taking data for elastic scattering and inelastic scattering to low-lying states and giant resonances of 240 MeV  ${}^6\text{Li}$  ions on  ${}^{24}\text{Mg}$ ,  ${}^{28}\text{Si}$ , and  ${}^{116}\text{Sn}$  [3]. Also, Krishichayan *et al.* showed that optical potential parameters for  ${}^6\text{Li}$  scattering calculated from systematics with respect to changing target mass number can be used to accurately calculate GMR cross-sections [4]. To demonstrate the effectiveness of the inverse kinematics measurement of the GMR, we measured  ${}^{28}\text{Si}$  and  ${}^{16}\text{O}$  stable nuclei for which the GMR is known. Additionally, we measured the GMR in  ${}^{18}\text{O}$ , and  ${}^{20}\text{Ne}$  stable nuclei for which the GMR is unknown and targets are difficult to make for normal kinematics studies

Nuclei excited to the GMR region are particle unstable and will decay by p,  $\alpha$  or n decay shortly after excitation. To reconstruct the event it is necessary to measure the energy and angle of the decay particle and of the residual heavy ion. In many lighter nuclei a few nucleons off stability, and in light proton rich nuclei, the neutron threshold is above the region of interest. There are 3 bodies in the final state (recoiling  ${}^6\text{Li}$ , decay particle, and residual heavy ion). The recoiling  ${}^6\text{Li}$  have low energy and for the most part will not get out of the target. Thus in order to experimentally determine the kinematics, we must measure at least three of the four quantities: decay particle energy and angle, and residual nucleus energy and angle. Thus a  $\Delta E$ - $\Delta E$ -E decay detector composed of plastic scintillator arrays has been built and tested to measure the energy and angle of the light decay particle. The heavy ion is measured using the Oxford detector in the MDM spectrometer. We can calibrate the decay detector elements using the EDSE model for scintillator light output [5]. A hole in the decay detector with a horizontal and vertical opening of  $5^\circ$  allows the residual heavy-ion to enter the MDM spectrometer, which has horizontal and

vertical angular acceptances of  $\pm 2.5^\circ$ . The energy and angle of the heavy-ion is determined with the Oxford detector. The decay detector can measure decay particles within an angular range of  $4^\circ$  to  $35^\circ$  with respect to the beam direction.

## II. Calibration Study of the Decay Detector

We had calibrated the decay detector with a beam of 30 MeV protons scattered from a  $^{12}\text{C}$  target. From data of the elastic scattering and inelastic scattering exciting the  $2^+$  (4.4 MeV) and  $3^-$  (9.6 MeV) levels of  $^{12}\text{C}$  [5], we were able to find a set of EDSE fit parameters ( $\rho$ , I, F) [6]; these parameters are intrinsic to the type of plastic scintillator used in all three layers of the detector. The last parameter, the normalization constant C, differs between all the strips and varies slightly according to the attenuation behavior along the length of each strip. Therefore, it is necessary to find the normalization constant C for  $\Delta\text{E}1$ ,  $\Delta\text{E}2$ , and E of all segments of the decay

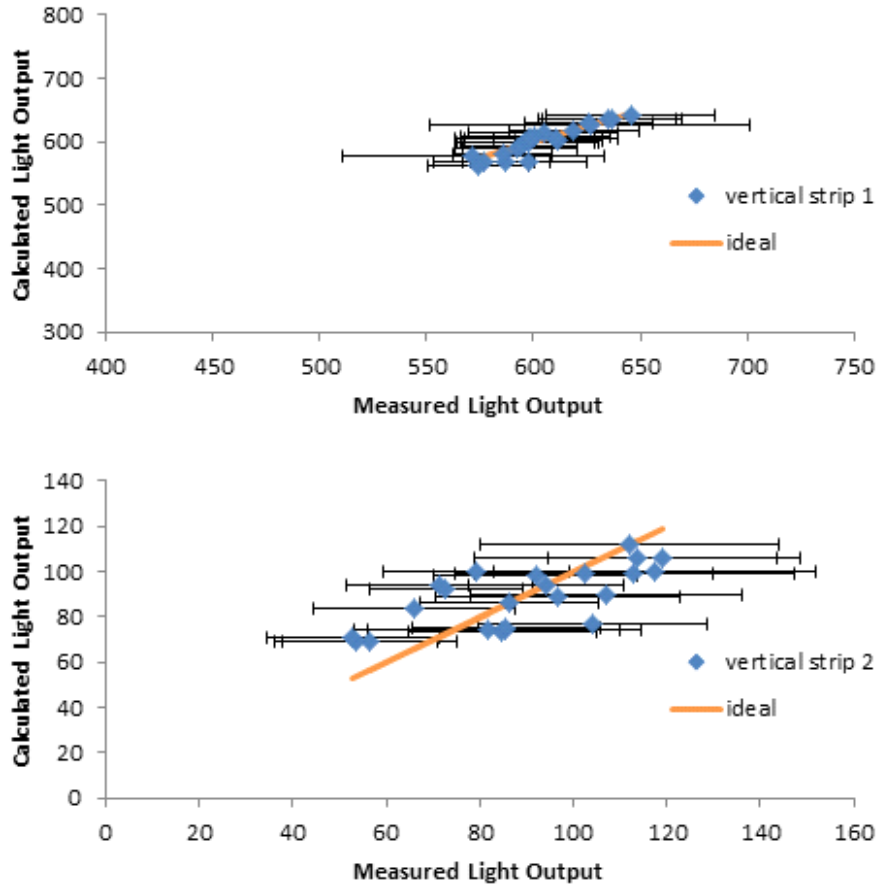


**FIG. 1.** Comparison of the measured and calculated light outputs of two of the vertical strips in the  $\Delta\text{E}1$  layer due to incident 15 MeV, 30 MeV, and 45 MeV protons and 100 MeV  $\alpha$ -particles from elastic scatter off  $^{12}\text{C}$  target: The calculated light output is obtained by using the EDSE model with these parameters obtained by  $\chi^2$  fit to the experimental data:  $\rho_1 = 373$  MeV/nm,  $F = 1$ , and  $A = 2.1\text{E-}5$ . The normalization constant, C, varies along the length of the vertical strip. The position on the vertical strip is determined by coincidence with the  $\Delta\text{E}2$  layer.  $C \approx 12.3$  for vertical strip 2, and  $C \approx 89.0$  for vertical strip 1

detector. Also the light output of the thin scintillator segments which are used in the two  $\Delta E$  layers of the decay detector may change over time so that a thorough calibration should be carried out shortly before each data run. All scintillators need to be handled carefully because applied pressure or torque will result in surface cracking (also known as crazing) and reduced efficiency of light transmission. The thin scintillators seem to be more prone to crazing than the scintillator blocks used in the E-layer.

Thus we did a series of calibrations using a  $^{12}\text{C}$  target with 15 MeV, 30 MeV, and 45 MeV proton beams and a 100 MeV  $\alpha$  beam earlier. Analysis of this calibration data is still ongoing. The procedure for obtaining the light response of the scintillator strips and blocks from the experimental data is outlined in Ref. [5]. The expected light response was calculated by first solving for the energy of the incident proton or  $\alpha$ -particle on  $\Delta E1$  using relativistic kinematics. The energy deposited in each layer was found by using the SRIM tables, and the EDSE model was used to calculate the expected light response. A comparison of the calculated and measured light outputs from the most recent calibration data is shown in Fig. 1.

### III. Faraday Cup and Blocker Plate

A movable Faraday cup and blocker plate were both installed in the space between the MDM Spectrometer and the Oxford detector. The cup consists of a thin layer of brass, in order to stop the beam, and a much thicker layer of tantalum to stop secondary decay particles. The horizontal positions of both the cup and plate can be controlled and read-out remotely. The cup, plate, and drive assembly can be seen in Fig. 2.

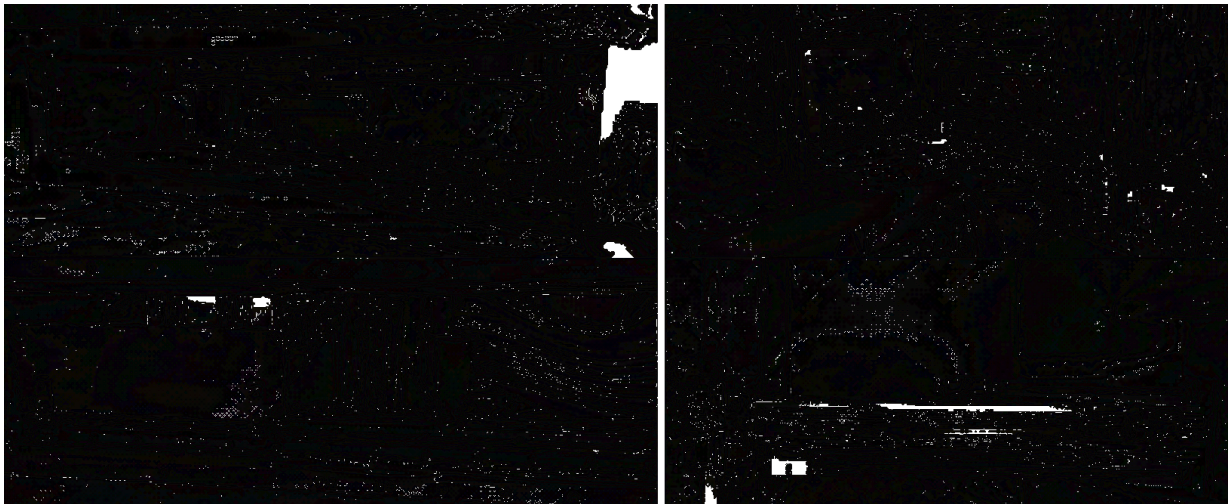


**FIG. 2.** From Top Left moving counter-clockwise: 1) Front-view of the Faraday Cup and Blocker Plate; 2) Back-view of the Cup and Plate, also visible are the tracks which span the length of the spacer section and that the two parts are mounted to; 3) Top-view of the exterior of the spacer section: There are two drive motors, the top motor moves the Cup and the bottom motor moves the Plate; 4) Side-view of the exterior of the spacer section.

The blocker plate completely covers entry into the Oxford detector and is intended to protect the detector from damage while tuning the beam onto the Faraday cup. The Faraday cup stops the beam near the focal plane but allows the heavy decay particle from GR excitation to enter into the detector on the left and right sides of the cup.

#### IV. Inverse Reaction Experiment

Data were taken using 40 MeV/u beams of  $^{28}\text{Si}$ ,  $^{16}\text{O}$ ,  $^{18}\text{O}$ , and  $^{20}\text{Ne}$  bombarding a  $^6\text{Li}$  target. Events were required to be coincident in the decay detector and in the Oxford detector. Signals from the  $\Delta E2$  layer were used as a trigger for gates to record signals from the  $\Delta E1$ ,  $\Delta E2$ , and E layers of the decay detector as well as the 4 proportional counter wires, cathode, and scintillator signals of the Oxford detector. An example illustrating how the new Faraday cup works to block the primary beam and allow the heavy residual ion from proton and  $\alpha$  decay can be seen in Fig. 3

When the detector calibration is completed, analysis of the inverse reaction data will

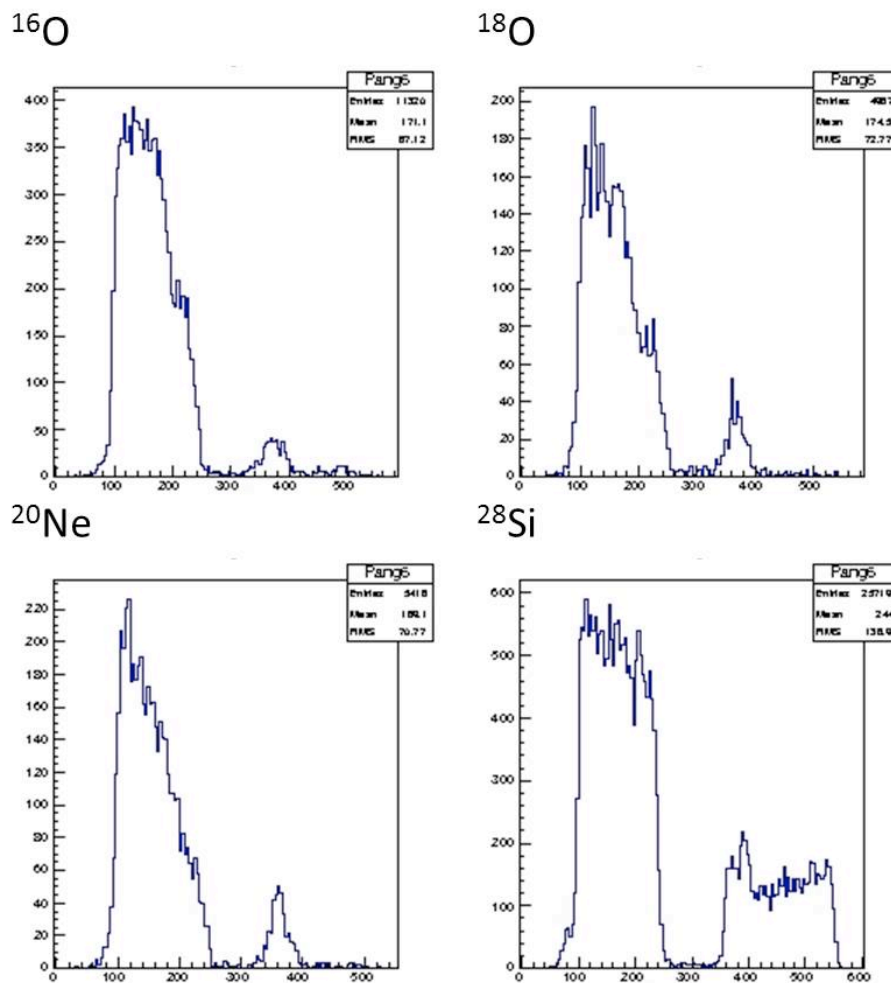


**FIG. 3.** The spectra for all heavy ions for an uncalibrated angle bin near  $0^\circ$  measured in the Oxford detector in coincidence with the decay detector. The gap in the middle of each spectrum correlates to the position of the Faraday cup before the Oxford detector. The low-side of each spectrum ( $<300$ ) corresponds to the heavy ion that results from proton decay, and the high-side corresponds to the heavy ion that results from  $\alpha$  decay

begin.

- [1] M. Harakeh and A. Van Der Woude, *Giant Resonances: Fundamental High-frequency Modes of Nuclear Excitation* (Clarendon Press, 2001).
- [2] E. Khan, Phys. Rev. C **80**, 011307 (2009).
- [3] X. Chen, Ph.D. Thesis, Texas A&M University, 2008.
- [4] Krishichayan, X. Chen, Y.-W. Lui, J. Button, and D. H. Youngblood, Phys.Rev.C **81**, 044612 (2010).
- [5] J. Button *et al.*, *Progress in Research*, Cyclotron Institute, Texas A&M University (2013-2014), p. IV-56.
- [6] K. Michaelian, A. Menchaca-Rocha, and E. Belmont-Moreno, Nucl. Instrum. Methods Phys. Res. A**356**, 297 (1995).